

## Original Research

# Longitudinal Anthropometric Assessment of Rhesus Macaque (*Macaca mulatta*) Model of Huntington Disease

Carissa E Hunter,<sup>1,2</sup> Alvince L Pongos,<sup>1</sup> Tim Y Chi,<sup>1,2</sup> Christa Payne,<sup>3</sup> Fawn C Stroud,<sup>4</sup> and Anthony W S Chan<sup>1,2,\*</sup>

The neurodegeneration associated with Huntington disease (HD) leads to the onset of motor and cognitive impairment and their advancement with increased age in humans. In children at risk for HD, body measurement growth abnormalities include a reduction in BMI, weight, height, and head circumference. The transgenic HD NHP model was first reported in 2008, and progressive decline in cognitive behaviors and motor impairment have been reported. This study focuses on longitudinal body measurements in HD macaques from infancy through adulthood. The growth of HD macaques was assessed through head circumference, sagittal and transverse head, and crown-to-rump ('height') measurements and BMI. The animals were measured monthly from 0 to 72 mo of age and every 3 mo from 72 mo of age onward. A mixed-effect model was used to assess subject-specific effects in our nonlinear serial data. Compared with WT controls, HD macaques displayed different developmental trajectories characterized by increased BMI, head circumference, and sagittal head measurements beginning around 40 mo of age. The physiologic comparability between NHP and humans underscores the translational utility of our HD macaques to evaluate growth and developmental patterns associated with HD.

**Abbreviations:** HD, Huntington disease; HTT, huntingtin

Huntington disease (HD) is an autosomal dominant disorder characterized by CAG trinucleotide repeat expansion in the *huntingtin* (*HTT*) gene. Expansions greater than 36 CAG repeats can lead to a prolonged polyglutamine stretch at the N-terminus of the HTT protein and, consequently, potential misfolding, aggregation, cellular dysfunction, and neural cell death.<sup>6,16</sup> The progressive neurodegeneration in HD is associated with symptoms including progressive deterioration of motor control and coordination, cognitive and psychiatric dysfunction, and death at 15 to 20 y after onset.<sup>3,7,9</sup> The age of onset strongly correlates with the length of the polyglutamine tract.<sup>6,9</sup> In adult-onset HD, patients usually have at least a 40Q expansion, and early symptoms begin between 35 and 50 y of age.<sup>9,18</sup>

Advancement in genetic engineering led to the production of the transgenic HD NHP model. HD does not naturally occur in NHP, with WT rhesus macaques containing 10 or 11 polyglutamine repeats. Transgenic NHP were first reported in 2008 and were generated by using lentiviruses overexpressing the human mutant *HTT* transgene.<sup>14,23</sup> Prior reports detailed progressive decline in cognitive behaviors and motor impairment that paralleled the human condition.<sup>24</sup>

In addition to motor impairment and cognitive decline, human HD patients experience weight loss and reduced BMI, and decreased head circumference is seen in preHD children,

compared with nonHD counterparts.<sup>11,15</sup> In the current study, we report the morphologic progression of body metrics of first-generation HD and WT male rhesus macaques from infancy through adulthood. The magnitude of data collected over the 100-mo monitoring period brings a unique opportunity to characterize growth trajectories and patterns of this HD model, a longitudinal assessment that has not been reported in humans. Here, we evaluate the BMI, head circumference, and—because of etiologic differences in head shape between humans and NHP—sagittal and transverse head measurements of HD macaques.

## Materials and Methods

**Animals.** All animal procedures (for example, housing, sample collection) were reviewed and approved by the IACUC of Emory University in accordance with the Animal Welfare Act and the *Guide for the Care and Use of Laboratory Animals* (8<sup>th</sup> edition).<sup>12</sup> Animals used for this study were rhesus macaques (*Macaca mulatta*). All subjects were born and reared under the same conditions. After their birth, infants were reared in a socially enriched nursery environment<sup>1,10,19</sup> at the Yerkes National Primate Research Center (Atlanta, GA), an AAALAC-accredited facility. Beginning at birth, all animals were observed at least twice daily by the research team, veterinary staff, or animal care personnel. Animals were fed commercial chow (Jumbo Monkey Diet 5037, Purina Mills, St. Louis MO) without restriction twice daily and seasonal fresh fruit and vegetables once daily.

**Subjects.** Longitudinal data were collected from 6 rhesus macaques born and located at the research center. Analysis was limited to first-generation male macaques with HD ( $n = 4$ ; rHD1, rHD6, rHD7, and rHD8) and their WT counterparts ( $n = 2$ ;

Received: 26 Jul 2017. Revision requested: 07 Sept 2017. Accepted: 18 Sep 2017.  
Division of <sup>1</sup>Neuropharmacology and Neurologic Diseases, <sup>2</sup>Department of Human Genetics, Emory University School of Medicine, Atlanta, Georgia, <sup>3</sup>Marcus Autism Center, Children's Healthcare of Atlanta, Department of Pediatrics, and <sup>4</sup>Division of Animal Resources, Yerkes National Primate Research Center, Emory University, Atlanta, Georgia

\*Corresponding author. Email: awchan@emory.edu

rWT1, rWT2). Nontransgenic WT controls were age-matched to and raised under the same conditions as HD animals. rHD1 contains a single copy of the human *HTT* exon 1, with 29Q and regulated by human polyubiquitin C promoter. rHD6, rHD7, and rHD8 each carry exons 1 through 10 of human *HTT* regulated by the human *HTT* promoter, with 67Q, 70Q, and 72Q, respectively.<sup>4</sup>

**Measurements.** BMI, head circumference, sagittal head measurement, and transverse head measurement were assessed monthly from birth until adulthood (72 mo) and then every 3 mo thereafter. Animals were anesthetized with 10 mg/kg ketamine for measurement. All measurements were taken by using the same nonstretch tape measure (in millimeters), calipers, and measurement protocols.

Head circumference was measured as the distance around the head, at the brow-line and above the ears. The sagittal head measurement was taken as the distance between eyes to the occiput. The transverse head parameter was the largest distance between the left and right sides of the head, measured just above and in front of the ears (Figure 1). Height was measured from crown to rump. Macaques were weighed in the morning, after an overnight fast. BMI was calculated as weight (kg)/height<sup>2</sup> (mm<sup>2</sup>); note that leg length was not included in the height component of this measurement.

**Model.** New studies underscore the utility of mixed-effects models to characterize growth curves from longitudinal data.<sup>13</sup> Mixed-effects regression is a mathematical method for hierarchical modeling, incorporating fixed and random effects. By using least-squares approximation, fixed effects are estimated parameters across all subjects. In contrast, random effects are estimated sample-dependent and subject-specific parameters, which help to enhance fit and reduce error in our model (Figure 2).

Previous studies in humans have shown that head circumference is a highly heritable trait and emphasized the importance of including subject-specific characteristics in head circumference analysis.<sup>5</sup> However, studies investigating head circumference have conflicting suggestions regarding the incorporation of height as a confounding variable to account for stature in the evaluation of head circumference.<sup>5</sup> The random-effects components allowed individualization of growth trajectories over time, thus accounting for variables like height and ancestry, which is important in light of our small sample size. Here, we report our mixed model and how it evaluates nonlinear, serial data.

The general form of a mixed-effects model is

$$y_{ij} = f(\phi_i, t_{ij}) + \varepsilon_{ij}.$$

For our analysis,  $y_{ij}$  is the BMI, head circumference, sagittal head measurement, or transverse head measurement of animal  $i$  at time  $j$ ;  $t_{ij}$  is the corresponding age (in months);  $\varepsilon$  is the corresponding error; and  $\phi_i$  is the set of regression coefficients, such that

$$\phi_i = (\alpha_0, \alpha_1, \alpha_2).$$

Each of the regression coefficients incorporates both fixed ( $\gamma$ ) and random effects ( $\beta$ ), such that

$$\alpha_{0j} = \gamma_0 + \beta_{0j}$$

$$\alpha_{1j} = \gamma_1 + \beta_{1j}, \text{ and}$$

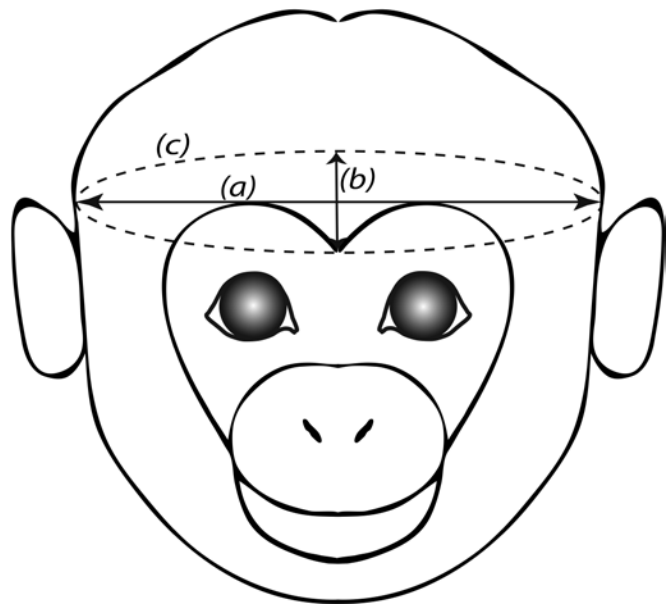


**Figure 1.** Sketch of macaque head indicating transverse head measurement (a), sagittal head measurement (b), and head circumference.

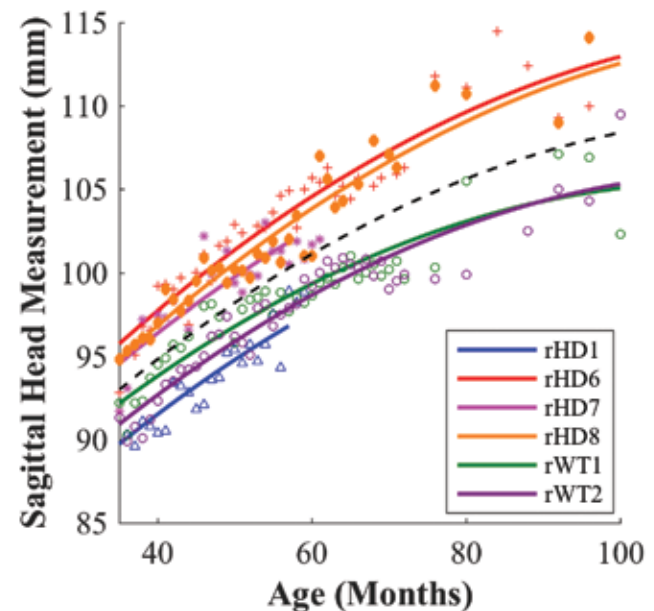


**Figure 2.** Sample curvilinear mixed model for head circumference. Fixed-effect curve (black) and random-effect curve (colors) for rHD1 (blue  $\Delta$ ), rHD6 (red +), rHD7 (pink \*), rHD8 (orange  $\diamond$ ), rWT1 (green o), and rWT2 (purple o). Fixed-effect curve indicates average growth of all animals, and random-effect curves are specific to respective animals.

$$\alpha_{2j} = \gamma_2 + \beta_{2j}.$$

A quadratic curvilinear fit was determined a posteriori by using the curve-fit tool of MATLAB (MathWorks, Natick, MA) and R-squared assessment, such that

$$y_{ij} = \alpha_{0j}(t^2) + \alpha_{1j}(t) + \alpha_{2j} + \varepsilon_{ij},$$

Where  $\varepsilon_{ij} \sim N(0, \sigma^2)$ . Independent from random-effect variables ( $\beta_{ij}$ ),  $\varepsilon$  was computed from our dataset by using MATLAB. We

confirmed normal distribution of our datasets through MATLAB's Jarque-Bera test (jbstest), where we returned  $h = 0$  to accept the null hypothesis of normal distribution for BMI, head circumference, sagittal head measurement, and transverse head measurement data sets.

In preliminary modeling with MATLAB's `nlmefit` function,  $\phi_i$  was found for each of the subjects in each of the mixed effects models. Due to the nature of the data collection, some variability exists in the measurement collection. Outliers were determined by using residual box plot, as data residing outside 99.3% normally distributed data.

Previous studies have shown the influence of birth weight on BMI progression.<sup>21</sup> Accordingly, we adjusted our random effects variance-covariance matrix in our BMI growth analysis to account for this effect, ultimately reducing error in our model. We used MATLAB's `nlmefit` function to run this mixed-effects regression.

Although we applied a nonlinear mixed effects regression method to reduce error and improve the fit of our growth models, a drawback of this method is comparing HD and WT beyond just confidence intervals. With one-way ANOVA, models resulted in comparable root mean-square errors. To compare growth trends, we ran one-way ANOVA  $F$  tests with MATLAB's `aoctool` algorithm.

## Results

Our nonlinear mixed-effects regressions modeled individualized growth trajectories, accounting for subject-specific characteristics in head circumference, head measurements, and BMI analyses. Residuals after mixed-effects regression had reduced error after accounting for random effects, confirming that this model successfully accounted for subject-specific characteristics. All WT confidence intervals were set to 99% (Figures 3 through 6). In addition, early sagittal and transverse head measurements on all animals (age, 0 to 29 mo) were inconsistent or inaccurate; we therefore began our analysis of these measurements at 30 mo of age.

Regarding BMI, head circumference, and sagittal head measurement, data from macaques rHD6 and rHD8 initially resided within the confidence intervals set by the measures from controls rWT1 and rWT2. However, an apparent shift occurred between 40 to 60 mo, where data for rHD6 and rHD8 fell outside the WT confidence intervals and showed a pronounced difference in growth trajectory (Figure 3 through 5).

Macaques rHD6 and rHD8 exhibited increased BMI for months 40 through 80, with a plateau at around 60 mo. Similarly, rHD7 approached the upper WT confidence interval at 50 mo and appeared to begin to depart from the WT growth trajectory for the last 10 mo (Figure 3). The head circumference mixed-effects regression showed that rHD6 and rHD8 diverged from the WT regression at 50 mo, whereas rHD1 and rHD7 followed the same trend as WT controls (Figure 3).

In addition, we observed different growth patterns of HD macaques between sagittal and transverse head measurements. The previously described divergence of rHD6 and rHD8 from WT is apparent in the sagittal head measurement, where animals rHD6, rHD7, and rHD8 began to show increased measurements during 40 to 60 mo (Figure 5). However, this prominent shift did not occur in the transverse head measurements (Figure 6). In contrast, animal rHD1 followed a different growth trajectory than macaques rHD6 through 8, which is most clearly evident in the sagittal head measurement and BMI mixed-effects regressions, where rHD1's measurement resided closely to the lower limit of the WT confidence interval. Overall, rHD1's

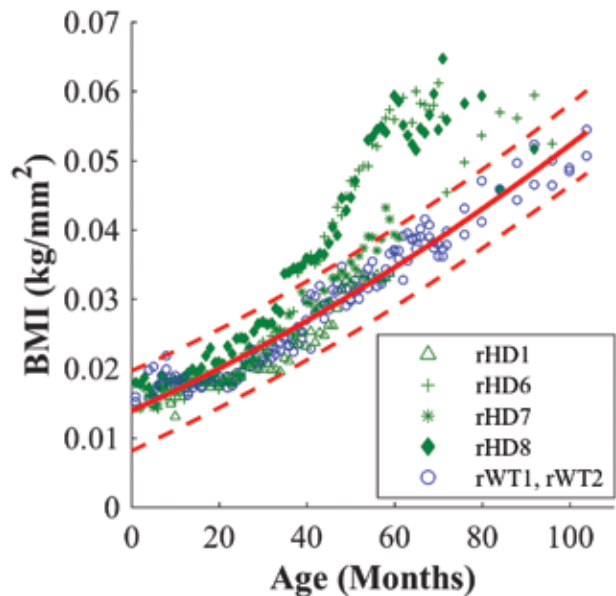


**Figure 3.** Mixed-effects regression for BMI of HD macaques (green) with fitted quadratic regression (solid red line) to WT macaques (blue). Red dotted lines indicate upper and lower 99% confidence intervals for WT macaques.

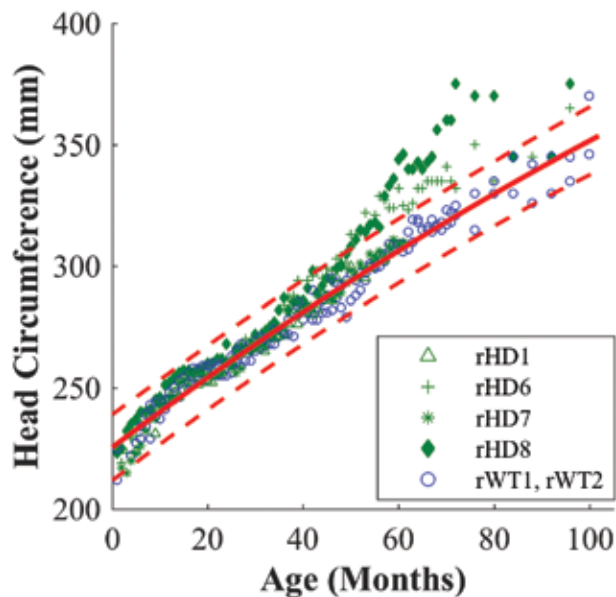


**Figure 4.** Mixed-effects regression for head circumference of HD macaques (green) with fitted quadratic regression (solid red line) to WT macaques (blue). Red dotted lines indicate upper and lower 99% confidence intervals for WT macaques.

measurements were lower than those of macaques rHD6 through 8 (Figure 3 and 5).

$F$  tests performed between WT controls and HD macaques (that is, rHD1, rHD6, rHD7, and rHD8) compared growth trajectories and rejected the null hypothesis that WT and HD groups were equal for each measurement. For BMI,  $F_{1,408} = 115.27$  ( $P < 0.0001$ ); for head circumference,  $F_{1,408} = 101.33$  ( $P < 0.0001$ ); for sagittal head measurement,  $F_{1,209} = 30.85$ ; ( $P < 0.0001$ ); and for transverse head measurement,  $F_{1,214} = 10.85$  ( $P < 0.005$ ).

## Discussion

In all analyses and discussion, we recognize the potential effects that our small sample size has regarding the findings of

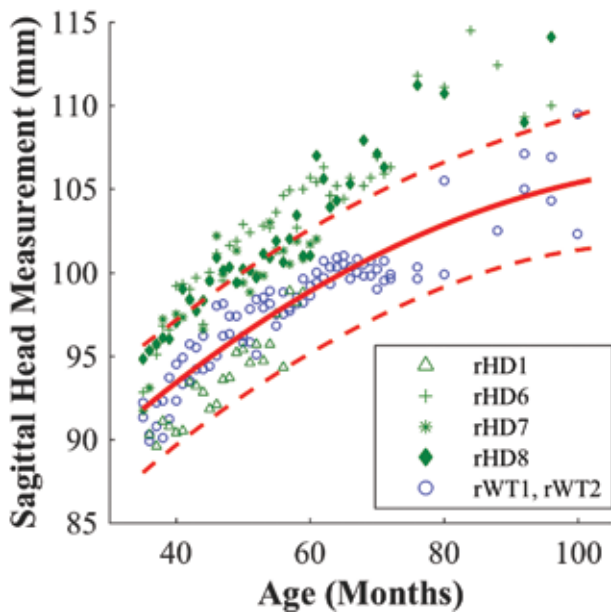


**Figure 5.** Mixed effects regression for sagittal head measurement of HD (green) with fitted quadratic regression (solid red line) to WT controls (blue). Red dotted lines indicate upper and lower 99% confidence intervals for WT macaques.

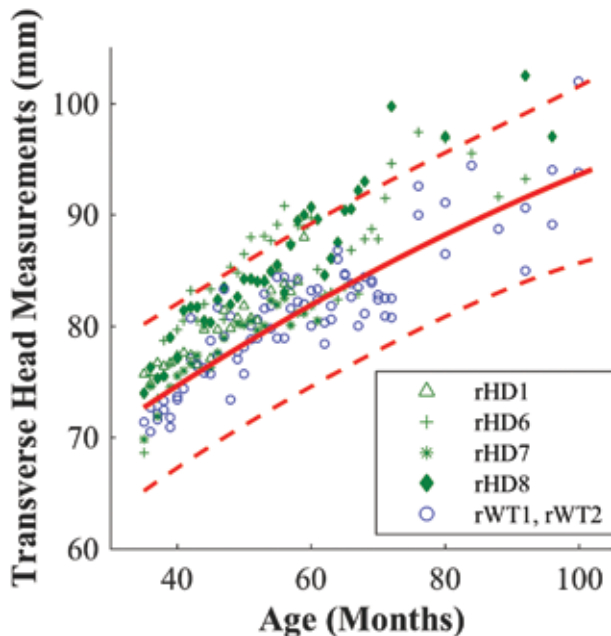


**Figure 6.** Mixed effects regression for transverse head measurement of HD (green) with fitted quadratic regression (solid red line) to WT controls (blue). Red dotted lines indicate upper and lower 99% confidence intervals for WT macaques.

different growth patterns and linear trajectories between HD and WT animals.

Both rHD6 and rHD8 showed marked increases in BMI relative to WT animals. Due to their weight-gain tendencies, both macaques have highly controlled diets and weight monitoring, which may account for the decrease and leveling of BMI around 80 mo of age (Figure 3). Metabolic disruption is shown consistently in human HD patients, but the specific changes in lipid and protein metabolites remain unclear.<sup>20</sup> Several theories address the cause of metabolic dysfunction in HD patients, including changes to diurnal hormones and deterioration of the parts

of the brain that control food intake.<sup>17</sup> The laboratory conditions of our animals control the variability in some aspects of metabolic profiling, such as diet and light:dark cycles. This reduction in variability, along with the reduced caloric usage due to constraints in the housing environment, might explain the consistent weight abnormalities in our HD animals. In the future, we would like to investigate the longitudinal metabolic profile of HD macaques by using blood samples collected throughout their lifespan.

Children at risk for HD have a decreased head circumference in comparison to that of healthy children.<sup>15</sup> In contrast, macaques rHD6 and rHD8 showed increased head circumference and sagittal head measurements when compared with WT animals. In addition, the transverse head measurement regressions showed a difference between the HD and WT animals, but it was not as marked as that of the sagittal head measurement (Figure 5 B). No known current studies investigate the relationship between sagittal head measurement and HD in humans, and this topic might warrant exploration.

The last measurement for rHD7 was at 61 mo of age, when he was euthanized for self-injurious behavior. Although his growth from 61 mo onward is unknown, we surmise that rHD7 would have followed the growth trajectory set by rHD6 and rHD8. Given the similarity in genotype of rHD7 to rHD6 and rHD8, it is unsurprising that his growth appears to approach and at times exceed the upper confidence interval set by the WT animals (Figures 3, 5, and 6 B). Macaque rHD1 exhibited the most aggressive development of HD.<sup>2</sup> His more severe phenotype might be responsible for deviation from the other HD growth trajectories and his markedly smaller head size, perhaps making him comparable in phenotype to juvenile HD in humans (Figures 3, 5, and 6 B).

The anomalous head measurements observed may implicate abnormal body development and growth.<sup>8</sup> Abnormal growth can be prompted by aberrant metabolic function, suggesting that metabolic dysfunction in HD animals is a contributing factor to the observed deviant body growth and BMI.<sup>15</sup> The extensive longitudinal data collected on the same animals at the same intervals may indicate a potentially important transition between 40 and 60 mo of age, when HD animals departed from the WT trend. This period is approximately the time when our animals were reaching sexual maturity. The developmental changes in hormone levels caused by puberty in HD animals might have influenced their metabolism and caused this shift.<sup>22</sup>

Expansion of the HD colony will reduce the uncertainty inherent with our limited number of HD animals. As we move forward, a larger sample size will lend itself to a comprehensive understanding and evaluation of male and female growth patterns, as well as first- and second-generation characteristics. In addition, ongoing measurements from second-generation animals will indicate whether growth patterns match trends of first-generation animals and lend insight into the effect of germline transmission on anthropometric measurements.

## Acknowledgments

We thank the YNPRC veterinarians and animal care staff. Special thanks to the veterinarian staff, primate enrichment team, and animal care personnel for providing superior medical and daily care to HD macaques as the disease progressed. We also thank current and past members of the Chan Lab team who contributed to the development of the HD NHP model. YNPRC is supported by the Office of Research and Infrastructure Program (ORIP)/OD P51OD11132. The Transgenic Huntington's Disease Monkey Resource (THDMR) and this study were supported by a grant awarded by the ORIP/NIH (OD010930) to AWSC.



## References

- Burbacher TM, Grant KS, Worlein J, Ha J, Curnow E, Juul S, Sackett GP. 2013. Four decades of leading-edge research in the reproductive and developmental sciences: the Infant Primate Research Laboratory at the University of Washington National Primate Research Center. *Am J Primatol* 75:1063–1083.
- Chan AW, Xu Y, Jiang J, Rahim T, Zhao D, Kocerha J, Chi T, Moran S, Engelhardt H, Larkin K, Neumann A, Cheng H, Li C, Nelson K, Banta H, Zola SM, Villinger F, Yang J, Testa CM, Mao H, Zhang X, Bachevalier J. 2014. A 2-y longitudinal study of a transgenic Huntington disease monkey. *BMC Neurosci* 15:1–11.
- Chan AWS. 2013. Progress and prospects for genetic modification of nonhuman primate models in biomedical research. *ILAR J* 54:211–223.
- Chan AWS, Jiang J, Chen Y, Li C, Prucha MS, Hu Y, Chi T, Moran S, Rahim T, Li S, Li X, Zola SM, Testa CM, Mao H, Villalba R, Smith Y, Zhang X, Bachevalier J. 2015. Progressive cognitive deficit, motor impairment, and striatal pathology in a transgenic Huntington disease monkey model from infancy to adulthood. *PLoS One* 10:1–16.
- Chaste P, Klei L, Sanders SJ, Murtha MT, Hus V, Lowe JK, Willsey AJ, Moreno-De-Luca D, Yu TW, Fombonne E, Geschwind D, Grice DE, Ledbetter DH, Lord C, Mane SM, Martin CL, Martin DM, Morrow EM, Walsh CA, Sutcliffe JS, State MW, Devlin B, Cook EH Jr, Kim SJ. 2013. Adjusting head circumference for covariates in autism: clinical correlates of a highly heritable continuous trait. *Biol Psychiatry* 74:576–584.
- Chen S, Ferrone FA, Wetzel R. 2002. Huntington's disease age-of-onset linked to polyglutamine aggregation nucleation. *Proc Natl Acad Sci U S A* 99:11884–11889.
- Crook ZR, Housman D. 2011. Huntington's disease: can mice lead the way to treatment? *Neuron* 69:423–435.
- Dunger DB, Ahmed ML, Ong KK. 2006. Early and late weight gain and the timing of puberty. *Mol Cell Endocrinol* 254–255:140–145.
- Gil JM, Rego AC. 2008. Mechanisms of neurodegeneration in Huntington's disease. *Eur J Neurosci* 27:2803–2820.
- Goursaud APS, Bachevalier J. 2007. Social attachment in juvenile monkeys with neonatal lesion of the hippocampus, amygdala, and orbital frontal cortex. *Behav Brain Res* 176:75–93.
- Hamilton JM, Wolfson T, Peavy GM, Jacobson MW, Corey-Bloom J, Huntington Study Group. 2004. Rate and correlates of weight change in Huntington's disease. *J Neurol Neurosurg Psychiatry* 75:209–212.
- Institute for Laboratory Animal Research. 2011. Guide for the care and use of laboratory animals, 8th ed. Washington (DC): National Academies Press.
- Johnson W, Balakrishna N, Griffiths PL. 2013. Modeling physical growth using mixed-effects models. *Am J Phys Anthropol* 150:58–67.
- Kocerha J, Liu Y, Willoughby D, Chidamparam K, Benito J, Nelson K, Xu Y, Chi T, Engelhardt H, Moran S, Yang S-H, Li S-H, Li X-J, Larkin K, Neumann A, Banta H, Yang JJ, Chan AWS. 2013. Longitudinal transcriptomic dysregulation in the peripheral blood of transgenic Huntington's disease monkeys. *BMC Neurosci* 14:1–10.
- Lee JK, Mathews K, Schlaggar B, Perlmutter J, Paulsen JS, Epping E, Burmeister L, Nopoulos P. 2012. Measures of growth in children at risk for Huntington disease. *Neurology* 79:668–674.
- MacDonald ME, Gines S, Gusella JF, Wheeler VC. 2003. Huntington's disease. *Neuromolecular Med* 4:7–20.
- Phan J, Hickey MA, Zhang P, Chesselet M-F, Reue K. 2009. Adipose tissue dysfunction tracks disease progression in 2 Huntington's disease mouse models. *Hum Mol Genet* 18:1006–1016.
- Quarrell OWJ, Nance MA, Nopoulos P, Paulsen JS, Smith JA, Squitieri F. 2013. Managing juvenile Huntington's disease. *Neurodegener Dis Manag* 3:267–276.
- Rommeck I, Capitano JP, Strand SC, McCowan B. 2011. Early social experience affects behavioral and physiological responsiveness to stressful conditions in infant rhesus macaques (*Macaca mulatta*). *Am J Primatol* 73:692–701.
- Skene DJ, Middleton B, Fraser CK, Pennings JLA, Kuchel TR, Rudiger SR, Bawden CS, Morton AJ. 2017. Metabolic profiling of presymptomatic Huntington's disease sheep reveals novel biomarkers. *Sci Rep* 7:1–16.
- Sørensen HT, Sabroe S, Rothman KJ, Gillman M, Fischer P, Sørensen TIA. 1997. Relation between weight and length at birth and body mass index in young adulthood: cohort study. *BMJ* 315:1137.
- Urbanski HF, Pau KYF. 1998. A biphasic developmental pattern of circulating leptin in the male rhesus macaque (*Macaca mulatta*). *Endocrinology* 139:2284–2286.
- Yang SH, Cheng PH, Banta H, Piotrowska-Nitsche K, Yang JJ, Cheng ECH, Snyder B, Larkin K, Liu J, Orkin J, Fang ZH, Smith Y, Bachevalier J, Zola SM, Li SH, Li XJ, Chan AWS. 2008. Towards a transgenic model of Huntington's disease in a nonhuman primate. *Nature* 453:921–924.